

# Crystallization Behavior of Polypropylene Filled with Surface-Modified Calcium Carbonate

KAZUTA MITSUISHI,\* SATORU UENO, SOUJI KODAMA, and HITOSHI KAWASAKI

Industrial Technology Center of Okayama Prefecture, 3-18 Ifuku-cho, 4 chome, Okayama 700, Japan

## SYNOPSIS

Polypropylene (PP) and calcium carbonate ( $\text{CaCO}_3$ ) were mixed in a two-roll mill. The mixed compounds were molded on the plate by using a compression press heater. To improve the affinity of the relation between  $\text{CaCO}_3$  and the PP matrix, we modified the  $\text{CaCO}_3$  surface through chemical reaction with alkyl dihydrogen phosphates. The  $\text{CaCO}_3$  content and size modification affected the crystallization behavior of the filled PP composites. The crystallization temperature in the nonisothermal crystallization process increased with the increase of  $\text{CaCO}_3$  content and the decrease of  $\text{CaCO}_3$  size. The crystallization temperature revealed the function of  $\log(1 + T_S)$  ( $T_S$ , total surface area of  $\text{CaCO}_3$ ) irrespective of  $\text{CaCO}_3$  content and size for modified and unmodified systems, respectively. The shoulder or double crystallization peak of PP composites is recognized for the unmodified system (particle sizes: 1.0 and 4.5  $\mu\text{m}$ ).

## INTRODUCTION

Nucleating agents are used to regulate the crystalline size in polypropylene molding. It is well known that the crystalline size affects the material characteristics, such as modulus and transmittance. Generally, the organic carboxyl salt and inorganic particle, etc., are applied to the polypropylene materials as the nucleating agents,<sup>1,2</sup> whereas the effectivity of inorganic particles on the polymer characteristics are used for mica,<sup>3</sup> calcium carbonate,<sup>4-6</sup> etc., to improve the mechanical properties, such as modulus and heat stability as well as the nucleating agents.

Recently, to improve the modulus and heat stability of polypropylene composites, inorganic particles (talc, mica, calcium carbonate, etc.) have generally been added to polypropylene, while Menczel et al.<sup>7</sup> related the effect of inorganic particles (talc) on the crystallization temperature and speed of polypropylene composites. Except for the study of the relation between inorganic particle size and content, modification for particle and crystallization behavior of polypropylene has not been systematically considered except for a short paper.<sup>8</sup>

Concerning the crystallization behavior of PP composites, Kowalewski and Galeski<sup>9</sup> reported on the effect of a modifier [poly(ethylene oxide)] for calcium carbonate on the crystallization of polypropylene composites. They reported that adding the modifier to polypropylene filled with calcium carbonate reduced the crystallization temperature of polypropylene composites in comparison to the unmodified system.

Hence, we have investigated the relation between particle size and content modification and the crystallization behavior of calcium carbonate-filled polypropylene.

## EXPERIMENTAL

### Materials

Isotactic polypropylene (PP, Showalomer, SA710, Showa Denko Co., MFI = 0.8, ASTM D 1238) was used as the polymer matrix. Calcium carbonate ( $\text{CaCO}_3$ , density = 2.7 g/cc, average particle sizes: 1.0, 4.5, and 30  $\mu\text{m}$ , see Table I, Bifoku Funka Kogyo Co.) was used as the filler for PP. The modifier for  $\text{CaCO}_3$  was alkyl dihydrogen phosphates (MAPn,  $\text{C}_n\text{H}_{2n+1}\text{OPO}(\text{OH})_2$ ,  $n = 1, 4, 10, 12, 16$ ).<sup>10</sup>

\* To whom correspondence should be addressed.

**Table I** Average Particle Size of CaCO<sub>3</sub>

	Average Size ( $\mu\text{m}$ )
F1	1.0
F4.5	4.5
F30	30.0

### Modification for CaCO<sub>3</sub>

First, the CaCO<sub>3</sub> particle was dried at 105°C for 2 h in an oven. Next, ethanol (500 mL), the CaCO<sub>3</sub> particle (100 g), and the modifier (3 g) were put into a round flask to modify the CaCO<sub>3</sub> particle surface using a rotary evaporator in vacuum. The surface-modified CaCO<sub>3</sub> particle was air-dried thoroughly at 105°C for 2 h.

### Mixing and Molding

PP and CaCO<sub>3</sub> particles were mixed in a two-roll mill (Kansai Roll Co., at 180 ± 5°C for 8 min). The PP mixture (filler content of 0.016, 0.032, 0.064, 0.09, 0.145, and 0.21 volume fraction) prepared by the mixing roll was pressed onto a molded plate by a compression press. A pressure of 14.7 MPa was used for 1 min after preheating at a temperature of 230 ± 2°C for 2 min. The molded plate was quenched by a cold press (the press temperature of iron plate is about 25 ± 5°C).

### DSC Measurement

Differential scanning calorimetry (DSC) measurements were performed with the DSC-20 (Seiko Denshi Kogyo Co.) apparatus. In the nonisothermal crystallization experiments, the samples were heated up to 200°C, kept at this temperature for 3 min, and then cooled down at 3°C/min to 100°C in nitrogen gas. During the cooling process, the crystallization patterns were recorded and crystallization temperature ( $C_T$ , peak temperature of crystallization) and crystallization enthalpy ( $\Delta H$  [mJ/mg]) were measured for the PP/CaCO<sub>3</sub> composites.

### Viscoelastic Test

The viscoelastic properties (loss tangent [ $\tan \delta$ ]) of CaCO<sub>3</sub>-filled PP composites were measured at a frequency of 50 Hz from -20 to 50°C, using a viscoelastic spectrometer ves-s (Iwamoto Seisakusho Co.).

### Tensile Test

The moduli of the samples were carried out for strip type (width 10 mm, length 50 mm) by using an Instron-type tensile machine (Tensilon UTM-II-20, Toyo Baldwin Co.) at the rate of 2 mm/min. The tensile impact strength for the unit cross-sectional area was measured by using an impact machine (Tensile Impact Tester, Toyo Seiki Co.).

## RESULTS AND DISCUSSION

### CaCO<sub>3</sub> Particle Size on Crystallization

The crystallization patterns of PP and PP/CaCO<sub>3</sub> composites are found to be Type I or Type II, as shown in Figure 1. The former type is a single peak and the latter type is a shoulder or double peak. Taking into account that the crystallization pattern of F1- and F4.5-filled PP is Type II, as shown in Table II, it was found that the CaCO<sub>3</sub> particle size has greatly influenced the crystallization temperature of the PP/CaCO<sub>3</sub> composites.

Figure 2 shows the relation between the  $C_T$  of PP and PP/CaCO<sub>3</sub> composites (unmodified) and the CaCO<sub>3</sub> volume fraction ( $\phi$ ). The value of  $C_T$  increases with  $\phi$  for all particle sizes. The measured data of  $C_T$  in Figure 2 is plotted for the lower temperature peak  $L_1$ . Here, the subscript of  $L$  shows the scanning times of DSC measurement. This phenomenon is attributed to the characteristics of the CaCO<sub>3</sub> particle on the crystallization of the PP matrix in the cooling process, which is concerned with the interaction of the polymer-particle interphase.

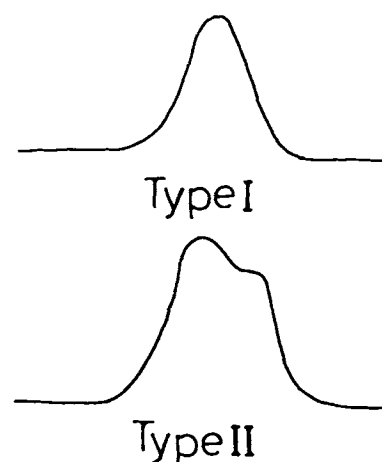


**Figure 1** DSC pattern of the PP/CaCO<sub>3</sub> system (non-isothermal crystallization).

**Table II Crystallization Temperature ( $C_T$ ) of Various Particle-Size CaCO<sub>3</sub>-Filled PP (CaCO<sub>3</sub> Volume Fraction is 0.145)**

	$C_T$ (°C)	
	High Temperature Peak	Low Temperature Peak
Average size (μm)		
1.0	124.4	121.5
4.5	121.7	119.5
30.0	—	117.6
PP	—	116.0

This is perhaps because the crystallization speed of the PP matrix has been changed by the interactive motion of the PP matrix layer at the particle surface. The activity of the particle surface increases with surface energy, which, in turn, increases with a decrease in particle size. The interaction of the polymer-particle interphase was reported in the previous paper,<sup>11</sup> in which we investigated the relation between the modulus and viscoelastic properties of CaCO<sub>3</sub>-filled PP and "the interactive index," which shows the interaction of the polymer-particle interphase and the factor of the interactive force, which contains the particle surface area, content, size, and size distribution. In these reports, we have shown that the modulus of the small-particle-filled PP composites is larger than that of the large-particle-filled PP.

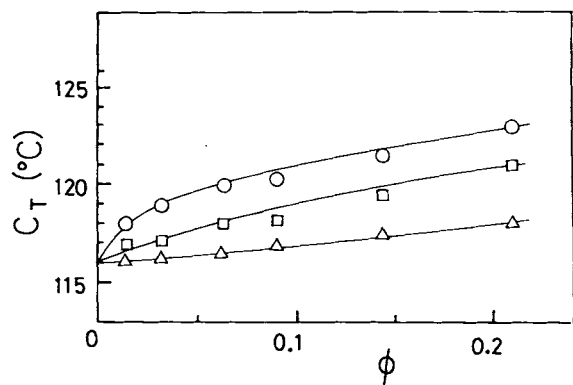


**Figure 2** Relation between  $C_T$  of various particle-size CaCO<sub>3</sub>-filled PP and CaCO<sub>3</sub> volume fraction ( $\phi$ ) of the unmodified system: (○) F1; (□) F4.5; (△) F30.

### Scanning Times and Crystallization

The polymer and inorganic particle are often mixed using the kneading machine, roll, banbury, etc. Hence, it is very important in a materials design system to investigate the relationship between thermohysteresis and crystallization behavior of PP/CaCO<sub>3</sub> composites as well as the mechanical properties of the composites. In this section, we investigate the effect of the repeating scanning times on the crystallization temperature of PP/CaCO<sub>3</sub> composites.

The relation between scanning times and the DSC pattern of F4.5 ( $\phi = 0.145$ ) is shown in Figure 3. In the first scanning, the higher peak  $H_1$  (121.7°C) and the lower peak  $L_1$  (119.5°C, shoulder peak) are detectable. To measure the crystalline phase of the  $H_1$  or  $L_1$  peak, X-ray diffraction measurements were applied to these samples. The results show that the (110), (040), (130), and (131) reflections are measurable for these samples, and here it is recognized that the  $H_1$  and  $L_1$  peaks are of the monoclinic system. Generally, when multiple peaks (e.g., two or three peaks) are present in the DSC pattern, these

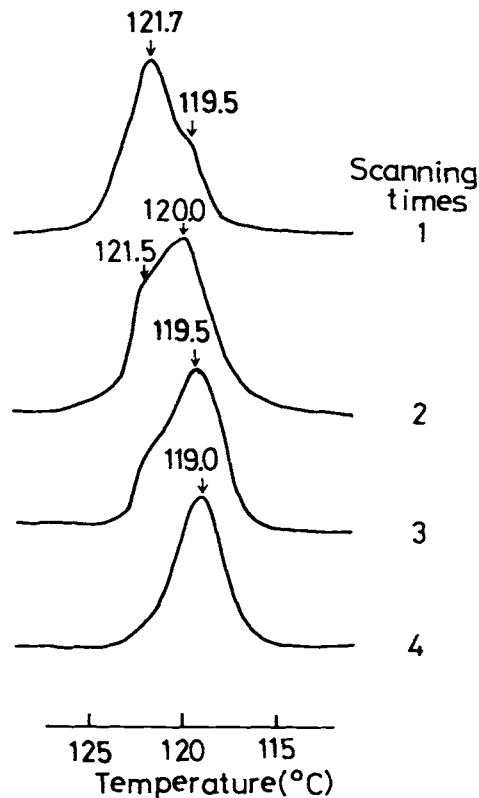


**Figure 3** DSC pattern of the PP/CaCO<sub>3</sub> (F4.5) system and scanning times.

peaks seem to indicate a crystalline transition of a different type and an annealing effect. But for the former reason, the mixture of different types of crystalline is not recognized in terms of the X-ray diffraction pattern in this experiment: consequently, these peaks have been recognized only as monoclinic crystalline. Further, these specimens are rapidly cooled by the cold press after compression using a press heater. From the appearance of these peaks (shoulder or double peak) for this case, the annealing effect for PP/CaCO<sub>3</sub> composites cannot be explained by the difference of these crystallization peaks. Hence, it seems that the appearance of these peaks in the PP/CaCO<sub>3</sub> composites is due to the addition of the CaCO<sub>3</sub> particle to the PP matrix. At the secondary scanning, the *L*<sub>2</sub> peak is relatively larger than the higher H<sub>2</sub> peak, and the higher peak gradually disappears with an increase of scanning time. Finally, the crystallization peak becomes the Li peak only.

Acosta et al.<sup>12,13</sup> have reported that the double peak is found in the DSC measurement, with the shoulder peak appearing at the lower temperature of PP filled with the sepiolite system. Moreover, these peaks indicate the presence of a "different ordered structure." Also, it is supposed that these peaks (the Hi and Li peaks) will be different crystallized peaks. Considering the above circumstances, the reasons for the irregular pattern is believed to be (i) the difference of crystallization behavior around the particle and the other parts and (ii) the presence of both accelerating and nonaccelerating crystallized parts on the particle surface, but this has not been confirmed.

Therefore, we attempted to evaluate the irregular crystallization pattern. It is suspected that the crystallization of the polymer matrix at the particle surface region has, first, advanced in comparison to the other parts (polymer region) and, consequently, the restriction of the polymer chain movement (namely "mesophase") at the surrounding particle has been affected by the crystallization of the polymer matrix

**Table III Scanning Times and Crystallization Enthalpy ( $\Delta H$ ) of CaCO<sub>3</sub> (F4.5,  $\phi = 0.145$ )-Filled PP**

Scanning Times	$\Delta H$ (mJ/mg)
1	65.7
2	63.4
3	60.0
4	60.2

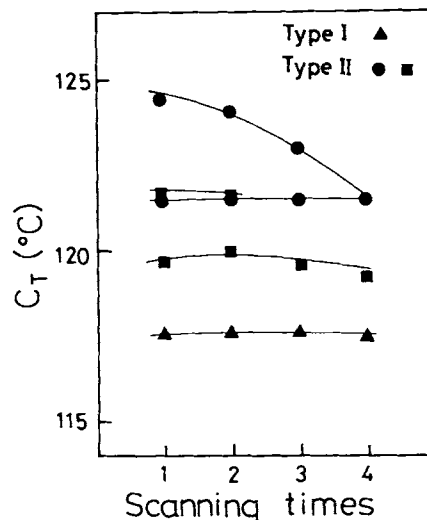


**Figure 4** Relation between  $C_T$  of various particle-size CaCO<sub>3</sub>-filled PP and scanning times ( $\phi = 0.145$ ), unmodified system: (●) F1; (■) F4.5; (▲) F30.

in the nonisothermal crystallization process. Hence, the crystallization behavior of the PP-CaCO<sub>3</sub> interphase seems to be developed on the irregular crystalline growth. As for this phenomenon, Chacko et al.<sup>14</sup> reported that the morphology of lamella at the polymer-particle interphase has changed in comparison to the other parts for polyethylene-CaCO<sub>3</sub> composites.

Table III shows the  $\Delta H$  of PP/CaCO<sub>3</sub> ( $\phi = 0.145$ , F4.5) composites against the scanning times. The value of  $\Delta H$  decreased with the increase of scanning times. The scanning times of the PP/CaCO<sub>3</sub> system have been found to affect the crystallization behavior, but we cannot explain the change of the  $\Delta H$  in this experiment. Maurer et al.<sup>15</sup> have reported that the presence of the "nonmelted region" at the polymer-particle interphase for polyethylene/kaolin composites is due to the reduction of  $\Delta H$ .

Figure 4 plots the  $C_T$  of various particle-size CaCO<sub>3</sub>-filled PP against the DSC scanning times. The DSC pattern of F1-, F4.5-, and F30-filled PP are of Types II, II, and I, respectively. The Hi peak temperature of F1 and F4.5 decreased with the increase of the scanning times, but the scanning-time dependence of the Li peak was not recognized.

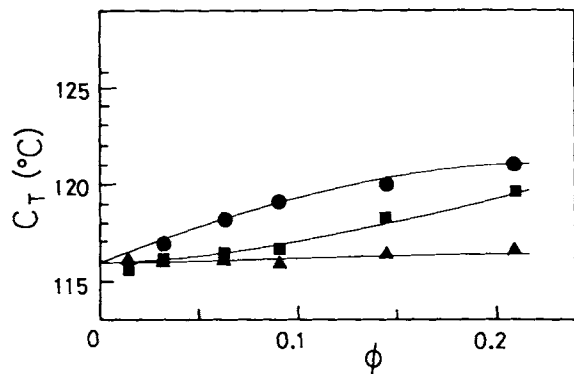
#### CaCO<sub>3</sub> Modification Effect on Crystallization

The crystallization temperature of PP generally affects the quality of injection moldings and films, in which the nucleating agents (alkyl carboxyl compound, talc, silica, etc.) can be applied to accelerate the crystallization of composites.

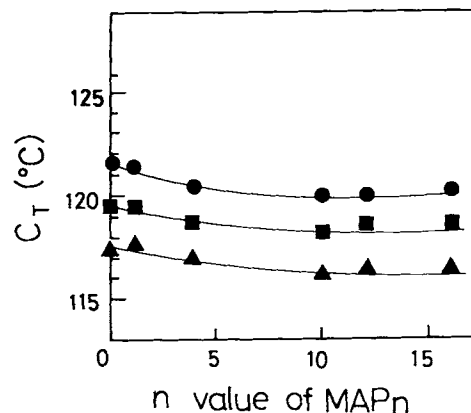
One of the important factors of crystallization effectivity for polymer products is attributed to the interactive adhesion of the organic or inorganic particle surface and polymer matrix. Hence, in this section, we discuss the relationship among the  $C_T$  of CaCO<sub>3</sub>-filled PP and  $\phi$ , CaCO<sub>3</sub> particle size, and the carbon number of alkyl dihydrogen phosphates [MAP $n$ , C $_n$ H $_{2n+1}$ OPO(OH) $_2$ ,  $n = 1, 4, 10, 12, 16$ ], as shown in Figures 5 and 6.

Figure 5 is a plot of the  $C_T$  of MAP4-modified CaCO<sub>3</sub>-filled PP and  $\phi$ . The CaCO<sub>3</sub> content dependence of the modified system is the same as that of the unmodified system for this experiment, but the value of  $C_T$  in the modified system is reduced in contrast to the unmodified system for same CaCO<sub>3</sub> content. This fact is due to the relaxation of the resistance of the polymer chain movement at the PP-CaCO<sub>3</sub> interphase and the restriction of rapid crystallization. Although the shoulder or double peak of PP/CaCO<sub>3</sub> composites is present for unmodified systems, it is not absent for the modified system. This is perhaps because of the existence of the MAP4 layer surrounding the CaCO<sub>3</sub> surface, in which the resistance of the PP molecular chain is relaxed (or plasticized) and the interactive movement of the polymer-particle interphase is reduced. Finally, the reduction of crystallization temperature of the PP/CaCO<sub>3</sub> system has been performed in terms of the combination of modified CaCO<sub>3</sub>.

Figure 6 shows the value of  $C_T$  against the carbon number of alkyl hydrogen phosphates ( $\phi = 0.145$ ). The dependence of carbon number on the crystallization temperature of PP composites is slight. The increase of carbon number gradually reduced the value of  $C_T$  in the PP/CaCO<sub>3</sub> composites and the value of  $C_T$  of MAP10 was the minimum value. Parrini and Corrieri<sup>16</sup> have previously reported that ad-



**Figure 5** Relation between  $C_T$  of various particle-size CaCO<sub>3</sub>-filled PP and CaCO<sub>3</sub> volume fraction ( $\phi$ ), MAP4 modified system: (●) F1; (■) F4.5; (▲) F30.



**Figure 6** Relation between  $C_T$  of various particle-size CaCO<sub>3</sub>-filled PP and  $n$  value of MAP $n$  ( $\phi = 0.145$ ): (●) F1; (■) F4.5; (▲) F30.

dition of a comparatively low molecular weight solvent for PP reduces the melting temperature.

In other words, the surface modification for CaCO<sub>3</sub> is important in evaluating the morphology and crystallization behavior of the PP-CaCO<sub>3</sub> interphase and the conformation change of the PP chain at the CaCO<sub>3</sub> surface.

#### Surface Area Effect on Crystallization Temperature

We have evaluated the  $C_T$  of PP composites against  $\phi$  for MAP $n$  modified and unmodified CaCO<sub>3</sub> systems. The physical properties of the particle (shape, surface area, etc.) as well as the chemical component feature are some of the important factors affecting the crystallization of the PP matrix.

Shibayama and Suzuki<sup>17</sup> have reported the assumption that the matrix restriction accompanying the adhesion between the particle and the polymer matrix can be determined by the chemical network:

$$T_g = K_1 \ln K_2 \psi \quad (1)$$

Iisaka<sup>18</sup> gave eq. (2), taking into account the surface area of the particle ( $S$ ) per weight of unit polymer instead of chemical network shown in eq. (1):

$$T_g = K_3 \ln S \quad (2)$$

where  $T_g$  is the transition temperature;  $\psi$ , the cross-link density of the polymer;  $S$ , the surface area per weight of unit polymer; and  $K_1$ ,  $K_2$ , and  $K_3$ , constant values.

The above equations have dealt with the network polymer, in which the  $T_g$  of polymer composites

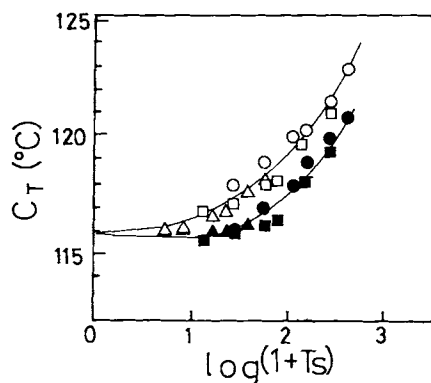


**Figure 7** Relation between  $C_T$  of various particle-size  $\text{CaCO}_3$ -filled PP and  $\log(1 + T_S)$ . MAP4 modified: (●) F1; (■) F4.5; (▲) F30. Unmodified: (○) F1; (□) F4.5; (△) F30.

generally increased with an increase in the network density and surface area, i.e.,  $T_g$  is dependent on the network density and the surface area of the particle. Hence, it is found that the crystallization of PP composites accelerated the interactive effect between the nucleating agent and the polymer matrix chain in the crystallization process, in which the melted PP matrix has rapidly (or slowly) cooled during the cooling process. Figure 7 is a plot of the  $C_T$  of the PP/ $\text{CaCO}_3$  system for the total surface area of  $\text{CaCO}_3$  ( $T_S$ ) and eq. (3) has been obtained:

$$C_T = K_4 \log(1 + T_S) \quad (3)$$

where  $K_4$  is the constant value. For unmodified and modified systems, the master curves are single lines irrespective of particle size and  $\phi$ , respectively, whereas the increment of  $C_T$  for  $\log(1 + T_S)$  of the MAP $n$  modified system is smaller than that of the unmodified one.

### Mechanical Properties and Crystallization Temperature

Figure 8 displays the loss tangent  $[(\tan \delta)_{\max}]$  of MAP4 modified and unmodified  $\text{CaCO}_3$ -filled PP against  $C_T$ . The value of loss tangent  $[(\tan \delta)_{\max}]$  shows the maximum value of  $\tan \delta$  for  $-20$  to  $50^\circ\text{C}$ . Generally, when the polymer matrix adheres strongly to the inorganic particle surface, it is well known that the  $\tan \delta$  of composites decreased with the increase of interaction force of the polymer-particle interphase. For the unmodified system, the value of  $(\tan \delta)_{\max}$  decreased with an increase of  $C_T$ . But for the MAP4 modified system, on the contrary, the value of  $(\tan \delta)_{\max}$  increased with  $C_T$ . Considering the above, for the crystallization be-

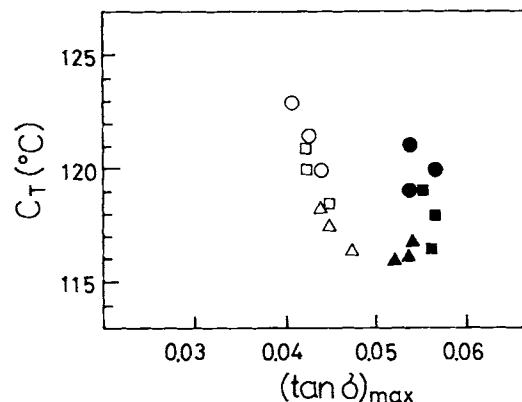


**Figure 8** Relation between  $C_T$  of various particle-size  $\text{CaCO}_3$ -filled PP and  $(\tan \delta)_{\max}$ . MAP4 modified: (●) F1; (■) F4.5; (▲) F30. Unmodified: (○) F1; (□) F4.5; (△) F30.

havior of the PP chain, it is believed that the modification of  $\text{CaCO}_3$  relaxed the restriction of the polymer-particle interphase, as the results  $[(\tan \delta)_{\max}]$  increased in comparison to unmodified system.

Figures 9 and 10 diagram the  $C_T$  against the relative modulus ( $E_c/E_p$ ,  $E_c$ , modulus of  $\text{CaCO}_3$ -filled PP;  $E_p$ , modulus of PP) and the relative impact strength ( $ISr$ ), respectively. Here, the value of  $ISr$  is given by

$$ISr = \frac{\text{(impact strength of the PP/CaCO}_3 \text{ system)}}{\text{(impact strength of PP)}}$$

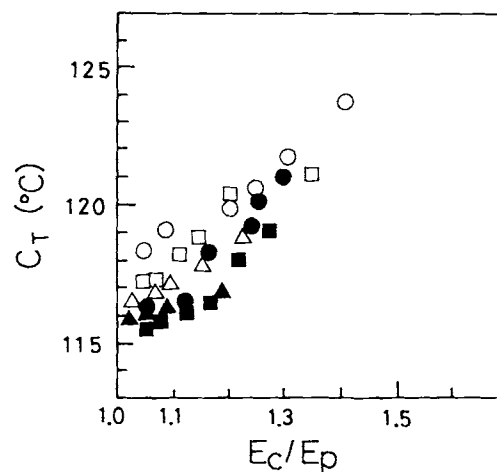


**Figure 9** Relation between  $C_T$  of various particle-size  $\text{CaCO}_3$ -filled PP and  $E_c/E_p$ . MAP4 modified: (●) F1; (■) F4.5; (▲) F30. Unmodified: (○) F1; (□) F4.5; (△) F30.

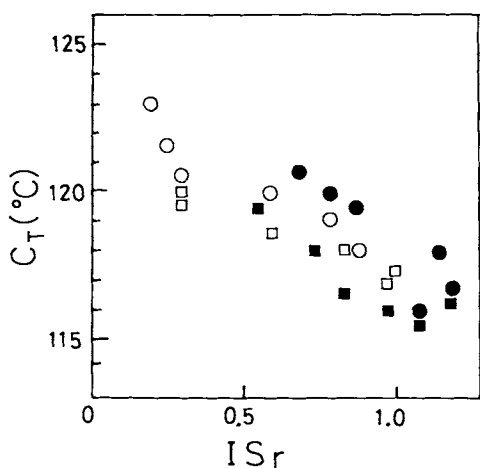


**Figure 10** Relation between  $C_T$  of various particle-size CaCO<sub>3</sub>-filled PP and  $ISr$ . MAP4 modified: (●) F1; (■) F4.5. Unmodified: (○) F1; (□) F4.5.

The larger the value of  $C_T$ , the larger the relative modulus is for the unmodified or modified system. Whereas the value of the  $ISr$  impact strength decreased with the increase of  $C_T$ , it is also shown that the crystallization temperature of PP/CaCO<sub>3</sub> is closely affected by the mechanical properties, such as modulus and impact strength.

When taken together, it shows that the increase of interaction at the polymer-particle interphase is concerned with the determination of the properties of PP/CaCO<sub>3</sub> composites in this experiment.

## CONCLUSIONS

The modification of calcium carbonate (CaCO<sub>3</sub>), CaCO<sub>3</sub> content, and size on the crystallization behavior (nonisothermal condition) of CaCO<sub>3</sub>-filled polypropylene was investigated. The obtained results are as follows:

1. The crystallization temperature in nonisothermal crystallization increased with the increase of CaCO<sub>3</sub> content and decrease of CaCO<sub>3</sub> size.
2. The crystallization temperature has revealed the function of  $\log(1 + T_S)$  ( $T_S$ , total surface

area of CaCO<sub>3</sub>) irrespective of CaCO<sub>3</sub> size and content for modified and unmodified systems, respectively.

3. The shoulder or double crystallization peak indicates the unmodified system (CaCO<sub>3</sub> particle sizes: 1.0 and 4.5  $\mu\text{m}$ ), but the pattern for the modified system remains as a single peak.

## REFERENCES

1. H. N. Beck and H. D. Ledbetter, *J. Appl. Polym. Sci.*, **9**, 2131 (1965).
2. H. N. Beck and H. D. Ledbetter, *J. Appl. Polym. Sci.*, **11**, 673 (1967).
3. C. Busigin, G. M. Martinez, R. T. Woodhams, and R. Lahtinen, *Polym. Eng. Sci.*, **23**, 766 (1983).
4. F. C. Naughton, *JAOCs*, **61**, 411 (1984).
5. P. L. Fernando, *Polym. Eng. Sci.*, **28**, 806 (1988).
6. A. Boldizar and J. Kubat, *Polym. Eng. Sci.*, **26**, 877 (1986).
7. J. Menczel and J. Varga, *J. Thermal Anal.*, **28**, 161 (1983).
8. T. J. Hutley and M. W. Darlington, *Polym. Commun.*, **26**, 264 (1985).
9. T. Kowalewski and A. Galeski, *J. Appl. Polym. Sci.*, **32**, 2919 (1986).
10. K. Mitsuishi, S. Kodama, H. Kawasaki, and M. Tanaka, *Chem. Express*, **2**, 281 (1987).
11. K. Mitsuishi, S. Kodama, H. Kawasaki, and M. Tanaka, *Polym. Prepr. Jpn.*, **36**, 1180 (1987).
12. J. A. Acosta, E. Morales, M. C. Ojeda, and A. Linares, *J. Mater. Sci.*, **21**, 725 (1986).
13. J. L. Acosta, C. M. Rocha, M. C. Ojeda, A. Linares, and M. Arroyo, *Angew. Makromol. Chem.*, **126**, 51 (1984).
14. V. P. Chacko, F. E. Kasasz, R. J. Farris, and E. L. Thomas, *J. Polym. Sci. Polym. Phys. Ed.*, **20**, 2177 (1982).
15. F. H. J. Maurer, R. Kosfeld, and Th. Uhlenbroich, *Colloid Polym. Sci.*, **263**, 624 (1985).
16. P. Parrini and G. Corrieri, *Makromol. Chem.*, **86**, 271 (1965).
17. Y. Shibayama and Y. Suzuki, *J. Polym. Sci. A*, **3**, 2637 (1965).
18. K. Iisaka, *Kobunshi Ronbunshu*, **33**, 427 (1976).

Received July 13, 1989

Accepted January 13, 1991